APPL1 negatively regulates bone mass, possibly by controlling the fate of bone marrow mesenchymal progenitor cells

By Yuan-Yu LIN[*1,†] and Lily Q. DONG[*2]

(Edited by Tatsuo SUDA, M.J.A.)

Abstract: Adiponectin is an adipokine that can exert a regulatory function on bone metabolism. However, there are many contradictions between clinical and pre-clinical studies on adiponectin. APPL1 is an adaptor protein that can interact with adiponectin receptors. In the current study, we found that knockout of the *Appl1* gene in male mice was associated with higher bone volume and numbers of trabeculae than in females or controls. The trabecular thickness, cortical thickness, ratio of bone volume/trabecular volume, cross-sectional bone area, and mean polar moment of inertia increased in *Appl1* KO mice compared with wild-type mice. The number of osteoblasts increased but the number of adipocytes decreased in *Appl1* KO mice. Knockdown of *Appl1* impaired adipogenesis in bone marrow-derived mesenchymal stem cells. Mineralization was increased by knockdown of *Appl1* during osteoblast differentiation. Data from differentiation-related genes showed results consistent with the *in vivo* effects. In summary, this study provides further clarification of the effect of the adiponectin signaling pathway on bone metabolism.

Keywords: adiponectin, APPL1, bone metabolism, micro-computed tomography analysis

Introduction

In pre-clinical studies, adiponectin signaling has been suggested to play a critical role in bone metabolism.[1)–10)] So far, the results of previous studies using adiponectin deficiency and over-expression in mice as models have shown contradictions. Some studies emphasized that adiponectin has a positive effect on bone development.[4)–7),10)] Over-expression of adiponectin by genetic manipulation or adenovirus transfection increased the bone volume and bone mineral density in mice.[4),6)] In addition, knockout of adiponectin produced consistent effects in both genders.[5),10)] Wu and colleagues demonstrated that knockout of adiponectin impaired trabecular bone formation in the distal femur, which may be mediated by decreases in bone resorption through central and peripheral mechanisms; increases in osteoblast differentiation through the central mechanism were also observed.[10)] In contrast, some studies indicated that adiponectin has a negative effect on bone formation.[1),2),8),9)] Increased levels of circulatory adiponectin had negative effects on bone mineral density and bone formation,[1),2)] and the opposite result was seen in adiponectin knockout mice.[8)]

In clinical research, studies relating circulating levels of adiponectin to bone parameters have been reported. Most of the clinical observations implied that adiponectin is negatively associated with bone mineral density and suggested that adiponectin is a negative regulator of bone metabolism.[11)–15)] Clinical studies showed an inverse relationship between adiponectin levels and bone mineral density. However, clinical observations can only determine association, and confounding factors may lead to inappropriate interpretation of results.

[*1] Department of Animal Science and Technology, National Taiwan University, Taipei, Taiwan.

[*2] Department of Cell Systems & Anatomy, The University of Texas Health San Antonio, San Antonio, TX, U.S.A.

[†] Correspondence should be addressed: Y.-Y. Lin, Department of Animal Science and Technology, National Taiwan University, No. 50, Ln. 155, Sec. 3, Keelung Road, Da'an District, Taipei 106, Taiwan (e-mail: yylin@ntu.edu.tw).

Abbreviations: ALP: alkaline phosphatase; APPL1: adaptor protein containing pleckstrin homology domain, phosphotryosine binding domain and leucine zipper motif; BS: bone surface; ES: eroded surface; FAS: fatty acid synthase; FBS: fetal bovine serum; Glut4: glucose transporter 4; MSC: mesenchymal stem cell; msx2: msh homeobox 2; μCT: micro-computed tomography; N.Ob: number of osteoblasts; N.Oc: number of osteoclasts; PPARγ: peroxisome proliferator-activated receptor γ; SREBP1: sterol regulatory element-binding protein 1; VOI: volume of interest.

doi: 10.2183/pjab.96.027

Our group has investigated the role of adiponectin receptor 1 in bone metabolism.[16] We found that adiponectin receptor 1 over-expression in mice yielded greater bone volume and numbers of trabeculae than in wild-type mice; this indicated that adiponectin receptor 1 is a critical factor for bone homeostasis. However, there are still many contradictions between the results of clinical and preclinical research.

Adaptor protein containing pleckstrin homology domain, phosphotryosine binding domain and leucine zipper motif (APPL1) was discovered using the cytoplasmic domain of AdipoR1 as bait to screen a yeast two-hybrid cDNA library derived from human brain.[17] Previous research identified APPL1 interaction with adiponectin receptors in mammalian cells and the interaction was stimulated by adiponectin. Saito's group demonstrated that APPL1 is required for insulin-stimulated glucose transporter 4 (Glut4) translocation in rat primary adipocytes and skeletal muscle.[18] *Appl1* knockdown inhibited insulin-stimulated glucose transport, Glut4 translocation, and protein kinase B (also known as Akt) phosphorylation.[18] Furthermore, APPL1 mediated adiponectin signaling by directly interacting with the adiponectin receptor and enhancing liver kinase B cytosolic localization through the protein phosphatase 2A–protein kinase Cζ signaling pathway.[19] APPL1 also activated the AMPK upstream kinase, Ca^{2+}/calmodulin-dependent protein kinase by activating phospholipase C.[20] However, research to explore the function of APPL1 in bone metabolism is limited. In the current study, we used *Appl1* knockout (KO) mice as a model to elucidate the role of APPL1 in bone metabolism.

Materials and methods

Generation of *Appl1* knockout mice. The procedure for *Appl1* KO mice generation was described previously.[21] An *Appl1*-deficient mouse embryonic stem cell line, in which the *Appl1* gene was trapped by the manipulation of a cDNA fragment encoding β-geo (containing the β-galactosidase and neomycin genes). To generate *Appl1* KO mice, the *Appl1* gene-trapped stem cells were microinjected into C57BL/6 blastocysts and chimeras were crossed with C57/BL6 mice. Animals were maintained on a 12-h light/dark cycle and had free access to standard chow and water. All protocols for animal use and euthanasia were reviewed and approved by The University of Texas Health San Antonio Animal Care and Use Committee and the Animal Care and Use Committee of National Taiwan University.

Micro-computed tomography analysis and histological examination. A micro-computed tomography (μCT) scanner (Skyscan 1076, BRUKER, Kontich, Belgium) was used to examine bone mineral density and the properties of trabecular bone. Femurs were collected and all muscle tissue was removed from the bone. The samples were scanned in 70% ethanol, with the following settings: 60 kV, 167 uA, Aluminum 0.5 mm filter, 0.70 rotation step, 4 frame averaging, 2000 × 1336 CCD, 700 msec exposure, and 10 micron voxel size. Scan time was 34 minutes. Three-dimensional analysis was done to obtain the number of trabeculae, trabecular separation, trabecular thickness, and cortical thickness. Trabecular bone analysis was conducted in the distal femur (metaphysis). The volume of interest (VOI) started 0.05 mm from the distal growth plate and continued proximally for 1.5 mm (150 slices). 3D analysis was performed in this region using an automated script. Cortical bone analysis was conducted on the midshaft (mid diaphysis). The midpoint of the VOI was centered at 55% of the total femoral length from the proximal end. The VOI had a height of 0.5 mm. 3D- and 2D-analyses were performed in the region of interest. The μCT measurements followed the guidelines for bone microstructure.[22] Representative images of a lateral view of femurs, cortical VOI, and trabecular VOI are shown in Fig. 1. Femurs were examined histologically for the number of osteoblasts/bone surface, number of osteoclasts/bone surface, eroded surface/bone surface and adipocyte number/mm^2. The measurements followed the standard nomenclature and symbols approved by the American Society for Bone and Mineral Research.

Isolation of bone marrow-derived mesenchymal stem cells (MSCs) and cell culture conditions. The collection of bone marrow-derived MSCs was described previously.[16] Bone marrow cells were flushed from the femurs and tibia of 8-week-old FVB/NJNarl mice after sacrifice. The epiphyseal ends were removed with scissors and marrow cells harvested by inserting a syringe needle (23-gauge) and flushing with α-MEM medium (M0894, Sigma-Aldrich, St. Louis, MO. U.S.A.) supplemented with 20% fetal bovine serum (FBS; Biological Industries, Kibbutz Beit Haemek, Israel). After gentle agitation, the pooled cells were seeded on plastic dishes at a density of 10^6 nucleated cells/cm^2. Incubation was at 37 °C with 5% CO_2 in air in a humidified chamber

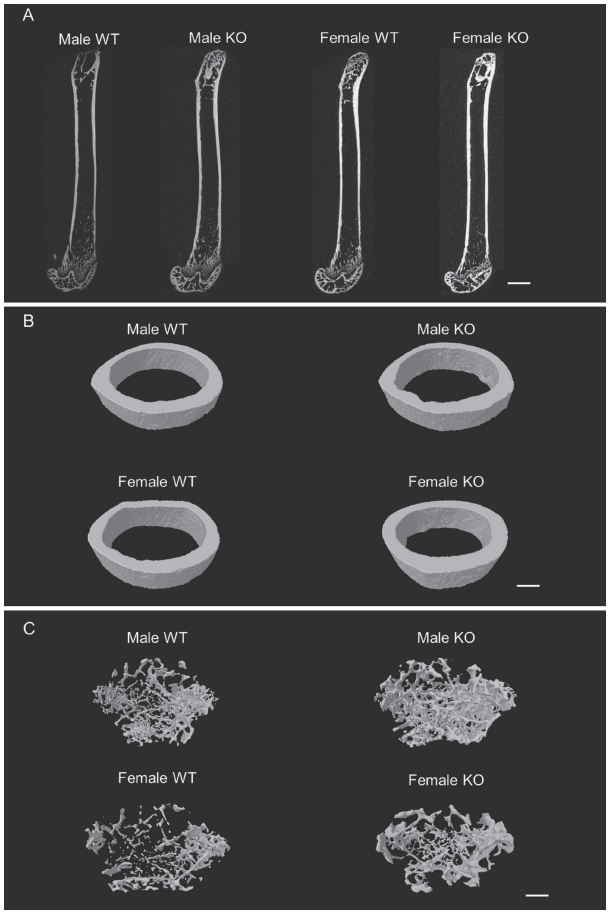

Fig. 1. Representative μCT images of mice of the indicated phenotype. (A) Femurs. (B) Cortical VOI. (C) Trabecular VOI. KO, *Appl1* knockout mouse; WT, wild-type mouse. Scale bar: 1 mm (1A); Scale bar: 250 μm (1B and 1C).

for 72 h. When the cells were nearly confluent, they were detached with 0.25% trypsin in 1 mM EDTA, and MSCs were purified from the heterogeneous cultured marrow cells using immuno-depletion protocols.[16] The bead-negative populations were washed and plated at a density of $10^5/cm^2$ for additional culture.

Lentivirus infection of *Appl1* shRNA into adipocytes and osteoblasts. MSCs were seeded at $8 \times 10^4/cm^2$ in 3 mL media on plates. Cells were seeded 1 day prior to infection and incubated for 16 h (37 °C in air containing 5% CO_2). Media were removed and fresh media containing polybrene (Sigma-Aldrich, H9268, St. Louis, MO. U.S.A.) and packaged lentivirus was added in accordance with the manufacturer's guidelines. Cells were incubated overnight (37 °C in air containing 5% CO_2). At 24 h post-infection, the culture media was removed and replaced with 3 mL of fresh α-MEM containing 8 μg/mL puromycin (Sigma-Aldrich, P8833). Puromycin selection requires at least 48 h of incubation. For adipocyte differentiation, puromycin-selected MSCs were incubated in adipogenic medium containing 10 μg/mL insulin (from bovine pancreas, Sigma-Aldrich), 1 μmol/L dexamethasone, 0.5 mmol/L 3-isobutyl-1-methylxanthine, 100 μmol/L indomethacin, and 10% FBS. The differentiation medium was changed every 3 days. Adipocytes were stained with Oil Red O (Sigma-Aldrich, O0625). For osteoblast differentiation, MSCs were incubated in osteogenic medium containing 10 mM glycerol-2-phosphate and 50 μg/mL ascorbate-2-phosphate. The cells were induced to differentiate at passage 2. Mineralized cells were stained with Alizarin Red S (Sigma-Aldrich, A5533). Control (pLAS.Void) and *Appl1* knockdown (KD) lentivirus (*Appl1* KD1: TRCN0000340759 and *Appl1* KD2: TRCN0000340817) were obtained from the National RNAi Core Facility of the Genomic Research Center (Academic Sinica, Taipei, Taiwan). *Appl1* KD1 and *Appl1* KD2 were two shRNA vectors with different sequences but with the same target in *Appl1* (both vectors were used).

RNA extraction and real-time PCR analysis. The methods for RNA extraction and real-time PCR were reported previously.[23] Total RNA was extracted from MSCs using the TRIzol Reagent (Invitrogen, Carlsbad, CA, U.S.A.) in accordance with the manufacturer's instructions. Samples were digested with DNase I (Ambion, Austin, TX, U.S.A.) at 37 °C for 30 min to remove genomic DNA interference and then reverse transcribed using a High Capacity cDNA Reverse Transcription kit (Applied Biosystems, CA, U.S.A.). The transcribed cDNA was amplified using a CFX96 Real-Time PCR Detection System (Bio-Rad, Richmond, CA, U.S.A.) and the end products were reacted with SYBR Green (Finnzymes, Espoo, Finland). Conditions for PCR reactions were initially denaturation at 95 °C for 7 min, followed by 39 cycles of denaturation at 95 °C for 10 s, annealing at 60 °C for 30 s. The mRNA levels of each gene were normalized using β-actin levels in the same sample and calculated using the formula of $(1/2)^{\text{Ct target genes} - \text{Ct } \beta\text{-actin}}$. Sequences of specific PCR primers for target gene amplification were as follows: β-actin, 5′-tgttaccaactgggacgaga-3′ (forward) and 5′-cttttcacggttggccttag-3′ (reverse); *Appl1*, 5′-aaacagcgttttcctttgggg-3′ (forward) and 5′-gcatgacaagaactaagctcatc-3′ (reverse); Osteocalcin, 5′-tagtgaacagactccggcgcta-3′ (forward) and 5′-

tgtaggcggtcttcaagccat-3′ (reverse); alkaline phosphatase (ALP), 5′-acactcggccgatcgggact-3′ (forward) and 5′-ccgccacccatgatcacgtcg-3′ (reverse); msh homeobox 2 (msx2), 5′-gaccagactccaggatggat-3′ (forward) and 5′-gcttagggtgacaatgcaag-3′ (reverse); sterol regulatory element-binding protein 1 (SREBP1), 5′-ggagccatggattgcacatt-3′ (forward) and 5′-ggcccgggaagtcactgt-3′ (reverse); peroxisome proliferator-activated receptor γ (PPARγ), 5′-gcctgcggaagccctttggt-3′ (forward) and 5′-aagcctgggcggtctccact-3′ (reverse); fatty acid synthase (FAS), 5′-ggaggtggtgatagccggtat-3′ (reverse) and 5′-tgggtaatccatagagcccag-3′ (reverse).

Enzyme-linked immunosorbent assay. Whole blood was obtained from wild-type and *APPL1* KO mice. Serum was collected by centrifugation for 15 min at approximately 2000 × g. Serum from wild-type and *APPL1* KO mice was used to measure the bone metabolism-related markers, osteocalcin (BT-479, Biomedical Technologies Inc., Stoughton, MA, U.S.A.) and TRAP5b (SB-TR103, MouseTRAP™ Assay, Immunodiagnostic Systems Inc., Scottsdale, AZ, U.S.A.) using the ELISA method.

Statistical analysis. All values were expressed as mean ± SEM. Results involving more than two groups were assessed using a one-way analysis of variance procedure. Tukey's test was used to evaluate differences among means (GraphPad Prism 5, Version 5.01, La Jolla, CA, U.S.A.). A significant difference was considered at $P \leq 0.05$.

Results

µCT analysis of *Appl1* knockout mice. In order to explore the role of *Appl1* in bone metabolism, we examined the bone volume and trabecular bone by µCT analysis in *Appl1* KO and wild-type mice. The trabecular bone volume fraction of the distal femur was greater in male *Appl1* KO mice than in female *Appl1* KO mice or controls of either gender (Fig. 2A). Trabecular thickness was higher in *Appl1* KO mice in both genders (Fig. 2B). Moreover, we quantified various traits of trabecular bone that showed the number of trabeculae was higher in male KO mice, but there was no change in trabecular separation (Fig. 2C and 2D). Cortical bone thickness was increased in both genders of *Appl1* KO compared with wild-type mice (Fig. 2E). We used the two dimensional bone area (a good indicator of the compressive strength of cortical bone tissue) to compare the bone strength between wild-type and *Appl1* KO mice. We found that the increased cortical thickness, along with slight increases in bone size, resulted in a large increase in mean polar moment; this suggested that the diaphysis was stronger in torsion (and most likely bending) in *Appl1* KO mice than in wild-type mice (Fig. 2E–2H). Representative

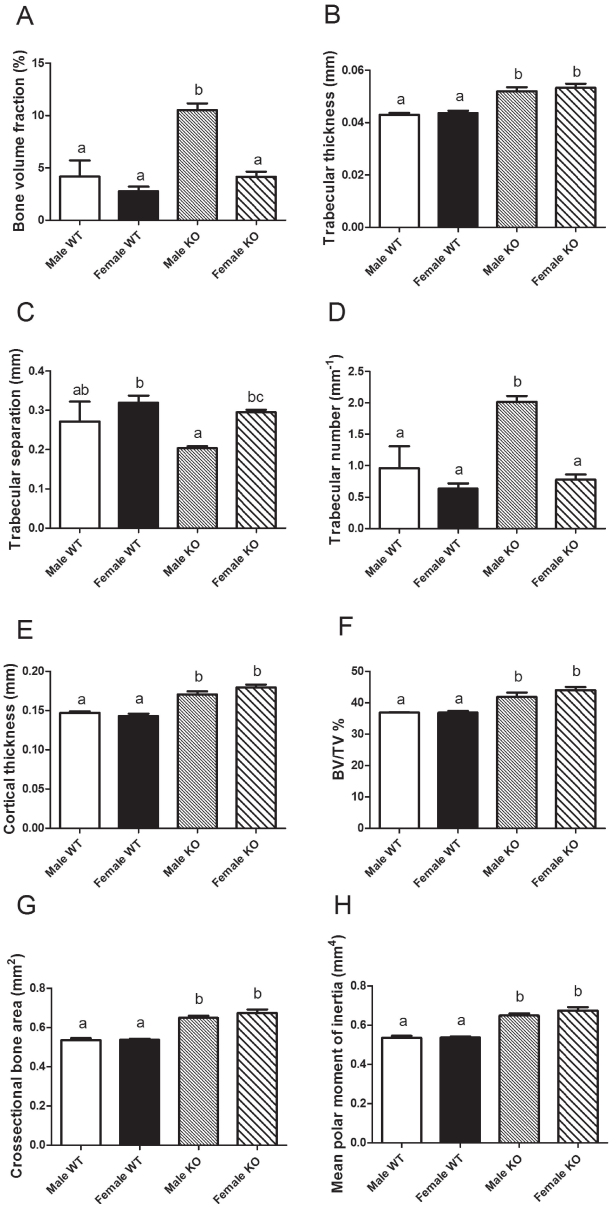

Fig. 2. µCT analysis of *Appl1* KO and WT mice. (A) Bone volume fraction. (B) Trabecular thickness. (C) Trabecular separation. (D) Number of trabeculae. (E) Cortical thickness. (F) Ratio of bone volume/trabecular volume. (G) Cross-sectional bone area. (H) Mean polar moment of inertia. KO, *Appl1* knockout mouse; WT, wild-type mouse. Data are expressed as mean ± SEM. n = 4/group. Different letters indicate $P \leq 0.05$.

images of the lateral view of femurs, cortical VOI, and trabecular VOI are shown in Fig. 1.

Expression of bone formation and resorption markers. Osteocalcin is an osteogenic marker that was increased in *Appl1* KO mice of both genders (Fig. 3A). Serum TRAP5b is a bone resorption marker that was not changed in *Appl1* KO mice compared with wild-type mice (Fig. 3B).

Bone histomorphometric analysis. *Appl1* KO mice had a greater number of osteoblasts/bone surface in both genders (Fig. 4A). The results of osteoclasts/bone surface and eroded surface/bone surface indicated that bone resorption may not have an impact in *Appl1* KO mice. This suggested that bone resorption may not be a factor in the current model (Fig. 4B and 4C). In addition, we found that the number of adipocytes per bone section was decreased in *Appl1* KO mice (Fig. 4D).

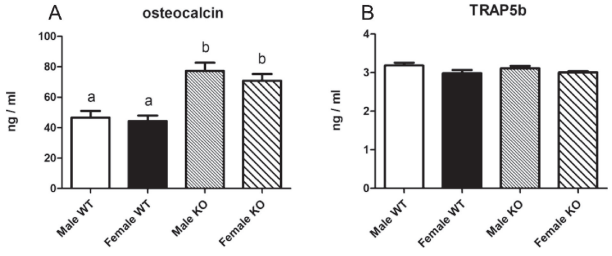

Fig. 3. Enzyme-linked immunosorbent assay from *Appl1* KO and WT mice. (A) osteocalcin. (B) TRAP5b. KO, *Appl1* knockout mouse; WT, wild-type mouse. Data are expressed as mean ± SEM. n = 4/group. Different letters indicate $P \leq 0.05$.

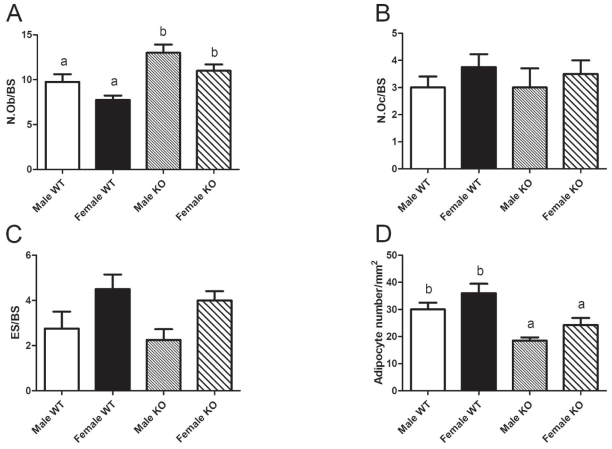

Fig. 4. Histological examination of bone tissue from *Appl1* KO and WT mice. (A) N.Ob/BS. (B) N.Oc/BS. (C) ES/BS. (D) Adipocyte number/mm^2. BS, bone surface; ES, eroded surface; KO, *Appl1* knockout mouse; N.Ob, number of osteoblasts; N.Oc, number of osteoclasts; WT, wild-type mouse. Data are expressed as mean ± SEM. n = 4/group. Different letters indicate $P \leq 0.05$.

Knockdown of *Appl1* expression impaired adipocytes differentiation in MSC. According to our current data *in vivo*, knockout of the *Appl1* gene in mice increased the ratio of bone volume/trabecular volume, trabecular thickness, and cortical thickness (Fig. 2). In order to investigate the role of *Appl1* in adipocyte and osteoblast differentiation in bone marrow, we isolated bone marrow-derived MSCs and impaired the *Appl1* gene by shRNA inhibition. At 24 h post-infection, the culture medium was removed and replaced with fresh growth medium containing 8 µg/mL puromycin. Puromycin-selected MSCs were incubated in adipogenic or osteogenic medium. The results showed that knockdown of the *Appl1* gene decreased the expression of *Appl1* by over 70% in MSCs (Supplementary Fig. 1). In addition, knockdown of *Appl1* not only decreased adipocyte differentiation, but also increased mineralization upon osteogenesis in MSCs (Fig. 5).

The marker genes for osteoblast differentiation, such as osteocalcin, ALP, and msx2 were increased in *Appl1* KD cells (Fig. 6A–C). In contrast, marker genes for adipocyte differentiation including PPARγ, SREBP1, and FAS were decreased in *Appl1* KD cells compared with control cells (Fig. 6D–F).

Discussion

In a previous study, we demonstrated that the lack of AdipoR1 impaired osteoblast differentiation and bone formation.[16] Adiponectin signaling is a critical factor for osteoblast differentiation and bone homeostasis. Based on previous studies, we specu-

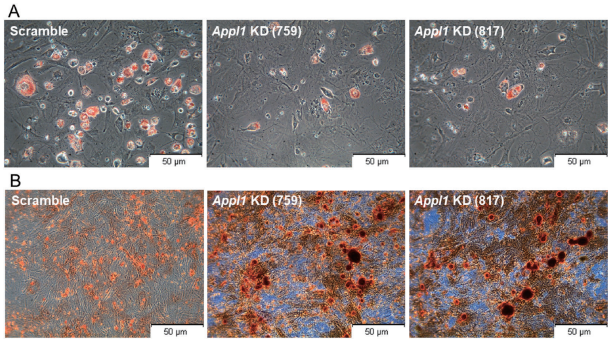

Fig. 5. Representative microscopic images of lentivirus-transfected MSCs during adipocyte and osteoblast differentiation. (A) Appearance of Oil Red O staining in lentivirus-transfected MSCs during adipocyte differentiation. (B) Appearance of Alizarin Red S staining in lentivirus-transfected MSCs during osteoblast differentiation.

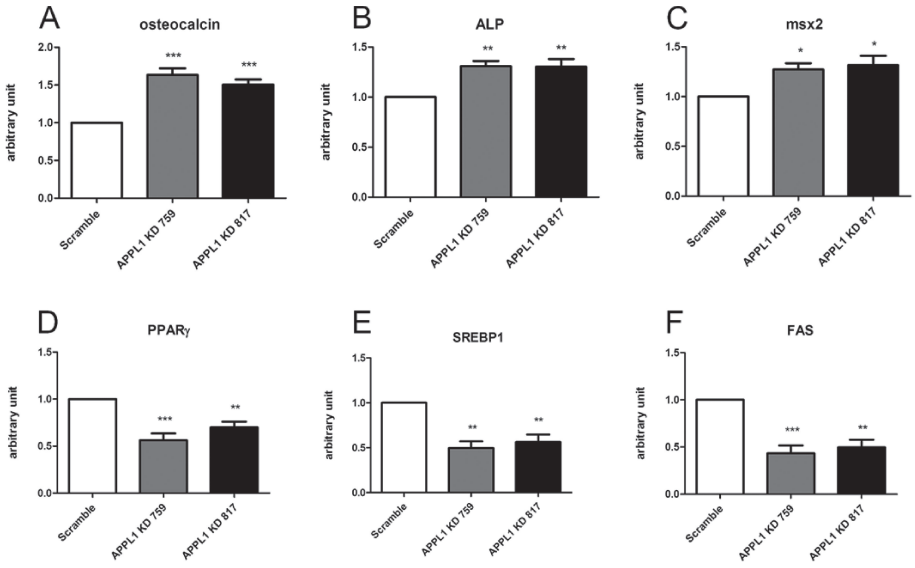

Fig. 6. Quantification of gene expression during adipocyte and osteoblast differentiation. (A) osteocalcin. (B) ALP. (C) msx2. (D) PPARγ. (E) SREBP1. (F) FAS. ALP, alkaline phosphatase; FAS, fatty acid synthase; msx2, msh homeobox 2; PPARγ, Peroxisome proliferator-activated receptor γ; SREBP1, sterol regulatory element-binding protein 1. mRNA levels were determined by real-time PCR and normalized to β-actin. Data are expressed as mean $\pm$ SEM. Symbols indicate statistical significance: *, $P \leq 0.05$; **, $P \leq 0.01$; and ***, $P \leq 0.001$ versus the scramble group n = 4/group.

lated that APPL1 has functions in bone development mediated by adiponectin signaling. The current results showed that KO of *Appl1* increased the bone volume fraction and number of trabeculae in male mice (Fig. 2A and 2D). Increases in trabecular thickness, cortical thickness, BV/TV%, cross-sectional bone area, and mean polar moment of inertia were observed in both genders of *Appl1* KO mice (Fig. 2B and 2E–2H). The cross-sectional bone area is the cortical bone equivalent area of the cross-section of the region of interest. The polar moment of inertia is used to quantify the resistance to deformation. The interaction between osteogenesis and adipogenesis within the bone marrow microenvironment is complex. Previous findings indicated that acceleration of bone marrow fat formation is associated with the progression of osteoporosis.[24] Bone marrow-derived adipocytes share the same progenitor cells with osteoblasts and chondrocytes and the concentration of the various progenitor cells in bone marrow are altered in various pathophysiological conditions. Therefore, we used adipocyte and osteoblast differentiation assays to verify the role of APPL1 in bone homeostasis. Retardation of *Appl1* decreased adipocyte differentiation and increased osteoblast mineralization, which may imply that *Appl1* is a negative regulator of bone formation (Fig. 5). A previous study claimed that APPL1 has positive effects on bone formation.[7] Bones explanted from adiponectin KO mice had reduced trabecular bone volume and cortical bone thickness. Increased number of osteoclasts have been reported in explanted bone from adiponectin KO mice.[7] It has been demonstrated that APPL1 promotes adiponectin signaling and is insulin-sensitizing.[21] On the other hand, insulin signaling also has been reported to be indispensable for bone formation by affecting both osteoblast and osteoclast development.[25] Our current model seems to conflict with the previous argument that insulin supports bone growth. However, there are novel factors related to adiponectin signaling that are not yet clarified regarding the molecular mechanisms of bone metabolism. First of all, there may be a compensatory effect of APPL proteins. APPL1 and APPL2 have a mutual compensation effect, which can affect the role of adiponectin and insulin signaling.[26] APPL2 can form a dimer with APPL1 to act as a negative regulator of adiponectin signaling.[26] Secondly, an alternative splicing variant of *Appl1* (*Appl1sv*) exerts an inhibitory function on hepatic adiponectin signaling and function.[3] Adenovirus-mediated short hairpin Appl1sv intervention was reduced in high fat diet-induced insulin resistance and hepatic glucose production in mice.[3] Therefore, the possibility of Appl1sv participation should not be ignored.

Thirdly, the hormone secreted from bone cells impacts the metabolism and bone turnover.[25] Osteocalcin and its receptor have critical roles in adiponectin signaling.[25),27] Adiponectin receptor 1 mediates the function of osteocalcin in glucose homeostasis in ovariectomized mice.[27] Based on the aforementioned studies, we speculate that these novel downstream molecules may also participate in bone metabolism. In summary, the contradictions or confounding factors between clinical research and pre-clinical research may also involve these molecules. The mechanism of APPL1 regulation of bone metabolism needs more supporting data.

In this study, we found that APPL1 may be a negative regulator of bone metabolism. The molecular mechanisms were beyond our current understanding regarding the roles of APPL1 in various physiological and pathological states and need further investigation.

Acknowledgments

The study was supported in part by MOST 106-2313-B-029-003-MY2 and 108-2313-B-002-062 grants from the Ministry of Science and Technology of Taiwan. We thank The University of Texas Health San Antonio for technical support with μCT analysis.

Supplementary material

Supplementary material is available at https://doi.org/10.2183/pjab.96.027.

References

1) Abbott, M.J., Roth, T.M., Ho, L., Wang, L., O'Carroll, D. and Nissenson, R.A. (2015) Negative skeletal effects of locally produced adiponectin. PLoS One **10**, e0134290.
2) Ealey, K.N., Kaludjerovic, J., Archer, M.C. and Ward, W.E. (2008) Adiponectin is a negative regulator of bone mineral and bone strength in growing mice. Exp. Biol. Med. **233**, 1546–1553.
3) Galan-Davila, A.K., Ryu, J., Dong, K., Xiao, Y., Dai, Z., Zhang, D. *et al.* (2018) Alternative splicing variant of the scaffold protein APPL1 suppresses hepatic adiponectin signaling and function. J. Biol. Chem. **293**, 6064–6074.
4) Mitsui, Y., Gotoh, M., Fukushima, N., Shirachi, I., Otabe, S., Yuan, X. *et al.* (2011) Hyperadiponectinemia enhances bone formation in mice. BMC Musculoskelet. Disord. **12**, 18.
5) Naot, D., Watson, M., Callon, K.E., Tuari, D., Musson, D.S., Choi, A.J. *et al.* (2016) Reduced bone density and cortical bone indices in female adiponectin-knockout mice. Endocrinology **157**, 3550–3561.
6) Oshima, K., Nampei, A., Matsuda, M., Iwaki, M., Fukuhara, A., Hashimoto, J. *et al.* (2005) Adiponectin increases bone mass by suppressing osteoclast and activating osteoblast. Biochem. Biophys. Res. Commun. **331**, 520–526.
7) Tu, Q., Zhang, J., Dong, L.Q., Saunders, E., Luo, E., Tang, J. *et al.* (2011) Adiponectin inhibits osteoclastogenesis and bone resorption via APPL1-mediated suppression of Akt1. J. Biol. Chem. **286**, 12542–12553.
8) Wang, Q.P., Li, X.P., Wang, M., Zhao, L.L., Li, H., Xie, H. *et al.* (2014) Adiponectin exerts its negative effect on bone metabolism via OPG/RANKL pathway: An in vivo study. Endocrine **47**, 845–853.
9) Williams, G.A., Wang, Y., Callon, K.E., Watson, M., Lin, J.M., Lam, J.B. *et al.* (2009) *In vitro* and *in vivo* effects of adiponectin on bone. Endocrinology **150**, 3603–3610.
10) Wu, Y., Tu, Q., Valverde, P., Zhang, J., Murray, D., Dong, L.Q. *et al.* (2014) Central adiponectin administration reveals new regulatory mechanisms of bone metabolism in mice. Am. J. Physiol. Endocrinol. Metab. **306**, E1418–E1430.
11) Barbour, K.E., Zmuda, J.M., Boudreau, R., Strotmeyer, E.S., Horwitz, M.J., Evans, R.W. *et al.* (2011) Adipokines and the risk of fracture in older adults. J. Bone Miner. Res. **26**, 1568–1576.
12) Biver, E., Salliot, C., Combescure, C., Gossec, L., Hardouin, P., Legroux-Gerot, I. *et al.* (2011) Influence of adipokines and ghrelin on bone mineral density and fracture risk: A systematic review and meta-analysis. J. Clin. Endocrinol. Metab. **96**, 2703–2713.
13) Kanazawa, I., Yamaguchi, I.T., Yamamoto, M., Yamauchi, M., Yano, S. and Sugimoto, T. (2009) Relationships between serum adiponectin levels versus bone mineral density, bone metabolic markers, and vertebral fractures in type 2 diabetes mellitus. Eur. J. Endocrinol. **160**, 265–273.
14) Michaelsson, K., Lind, L., Frystyk, J., Flyvbjerg, A., Gedeborg, R., Berne, C. *et al.* (2008) Serum adiponectin in elderly men does not correlate with fracture risk. J. Clin. Endocrinol. Metab. **93**, 4041–4047.
15) Napoli, N., Pedone, C., Pozzilli, P., Lauretani, F., Ferrucci, L. and Incalzi, R.A. (2010) Adiponectin and bone mass density: The InCHIANTI study. Bone **47**, 1001–1005.
16) Lin, Y.Y., Chen, C.Y., Chuang, T.Y., Lin, Y., Liu, H.Y., Mersmann, H.J. *et al.* (2014) Adiponectin receptor 1 regulates bone formation and osteoblast differentiation by GSK-3β/β-catenin signaling in mice. Bone **64**, 147–154.
17) Mao, X., Kikani, C.K., Riojas, R.A., Langlais, P., Wang, L., Ramos, F.J. *et al.* (2006) APPL1 binds to adiponectin receptors and mediates adiponectin signalling and function. Nat. Cell Biol. **8**, 516–523.
18) Saito, T., Jones, C.C., Huang, S., Czech, M.P. and Pilch, P.F. (2007) The interaction of Akt with APPL1 is required for insulin-stimulated Glut4 translocation. J. Biol. Chem. **282**, 32280–32287.
19) Deepa, S.S., Zhou, L., Ryu, J., Wang, C., Mao, X.,

Li, C. *et al.* (2011) APPL1 mediates adiponectin-induced LKB1 cytosolic localization through the PP2A-PKC ζ signaling pathway. Mol. Endocrinol. **25**, 1773–1785.
20) Zhou, L., Deepa, S.S., Etzler, J.C., Ryu, J., Mao, X., Fang, Q. *et al.* (2009) Adiponectin activates AMP-activated protein kinase in muscle cells via APPL1/LKB1-dependent and phospholipase C/Ca^{2+}/Ca^{2+}/calmodulin-dependent protein kinase kinase-dependent pathways. J. Biol. Chem. **284**, 22426–22435.
21) Ryu, J., Galan, A.K., Xin, X., Dong, F., Abdul-Ghani, M.A., Zhou, L. *et al.* (2014) APPL1 potentiates insulin sensitivity by facilitating the binding of IRS1/2 to the insulin receptor. Cell Rep. **7**, 1227–1238.
22) Bouxsein, M.L., Boyd, S.K., Christiansen, B.A., Guldberg, R.E., Jepsen, K.J. and Muller, R. (2010) Guidelines for assessment of bone microstructure in rodents using micro-computed tomography. J. Bone Miner. Res. **25**, 1468–1486.
23) Lin, Y.Y., Chen, C.Y., Lin, Y., Chiu, Y.P., Chen, C.C., Mersmann, H.J. *et al.* (2013) Modulation of glucose and lipid metabolism by porcine adiponectin receptor 1-transgenic mesenchymal stromal cells in diet induced obese mice. Cytotherapy **15**, 971–978.
24) Meunier, P., Aaron, J., Edouard, C. and Vignon, G. (1971) Osteoporosis and the replacement of cell populations of the marrow by adipose tissue. A quantitative study of 84 iliac bone biopsies. Clin. Orthop. Relat. Res. **80**, 147–154.
25) Pramojanee, S.N., Phimphilai, M., Chattipakorn, N. and Chattipakorn, S.C. (2014) Possible roles of insulin signaling in osteoblasts. Endocr. Res. **39**, 144–151.
26) Wang, C., Xin, C.X., Xiang, R., Ramos, F.J., Liu, M., Lee, H.J. *et al.* (2009) Yin-Yang regulation of adiponectin signaling by APPL isoforms in muscle cells. J. Biol. Chem. **284**, 31608–31615.
27) Lin, Y.Y., Chen, C.Y. and Ding, S.T. (2017) Adiponectin receptor 1 resists the decline of serum osteocalcin and GPRC6A expression in ovariectomized mice. PLoS One **12**, e0189063.

(Received June 3, 2020; accepted July 15, 2020)